

Electrostatic Tuning of the Proximity-Induced Exchange Field in EuS/Al Bilayers

T. J. Liu, J. C. Prestigiacomo, and P. W. Adams

Department of Physics and Astronomy, Louisiana State University, Baton Rouge, Louisiana 70803, USA
(Received 13 November 2012; revised manuscript received 1 May 2013; published 9 July 2013)

We demonstrate that the proximity-induced exchange field H_{ex} in ferromagnetic-paramagnetic bilayers can be modulated with an electric field. An electrostatic gate arrangement is used to tune the magnitude of H_{ex} in the Al component of EuS/Al bilayers. In samples with $H_{\text{ex}} \sim 2$ T, we were able to produce modulations of ± 10 mT with the application of perpendicular electric fields of the order of $\pm 10^6$ V/cm. We discuss several possible mechanisms accounting for the electric field's influence on the interfacial coupling between the Al layer and the ferromagnetic insulator EuS, along with the prospects of producing a superconducting field-effect transistor.

DOI: [10.1103/PhysRevLett.111.027207](https://doi.org/10.1103/PhysRevLett.111.027207)

PACS numbers: 75.70.-i, 74.78.-w, 85.25.-j, 85.80.Jm

The development of a magnetic analog of the ubiquitous field-effect transistor (FET) has been a long-term goal of the materials research community. Indeed, the electrical manipulation of magnetism is central to the future development of spintronic applications [1–5]. In contrast to semiconducting FETs, which use gate-controlled electric fields to modulate a device's charge carrier concentration, a magnetic FET would use a gate to modulate the magnetism of a thin magnetic film. Recently, gating strategies have been employed to tune the magnetic properties in complex multiferroics and ferromagnetic semiconductors [3,4,6–10]. In these studies, a magnetoelectric (ME) effect typically arises from the strain induced by the electric field and/or from the modulation of the carrier density itself. More complex strategies for the electric control of magnetism have also shown some success. These include using spin currents to produce torques on the magnetization vector [11,12] or, more recently, using electric field-induced ionic displacements to modulate the exchange bias in $\text{BiFeO}_3\text{-La}_{0.7}\text{Sr}_{0.3}\text{MnO}_3$ nanostructures [13]. In this Letter, we focus on ME effects that arise at the interface between a ferromagnetic insulator (FI) and an elemental paramagnet (PM). We employ a bilayer configuration in which a PM film is in intimate contact with the FI film. The exchange interaction between local magnetic moments in the FI and PM conduction electrons gives rise to a large effective internal field in the PM layer. This effective field, which only manifests itself through a Zeeman splitting of the PM conduction electrons, is commonly known as the exchange field H_{ex} [14–16]. Using a MOSFET-type geometry, we demonstrate that an exchange field of the order of several Tesla can be modulated by a few percent with gate voltages $\sim \pm 5$ V. We exploit this effect to tune the superconducting transition of the Al layer electrostatically.

The FI-PM bilayers were fabricated via *e*-beam deposition from EuS, SiO_x , and Al targets. A schematic of the sample geometry is shown in Fig. 1. First, a 10-nm-thick Al gate was deposited at room temperature through a mask onto fire-polished glass substrates. Then, a barrier layer of

50-nm-thick amorphous insulating SiO_x ($1 < x < 2$) was deposited on the gate. Using a different mask, a 5-nm-thick EuS film was deposited on top of the barrier layer at 84 K. Finally, the film of interest, a 2–3-nm-thick Al layer, was deposited on top of the EuS without breaking vacuum. To avoid leakage current at the edges, the area of the SiO_x barrier layer was slightly larger than that of the bilayer strip. The depositions were performed in a 4×10^{-7} torr vacuum at a rate of ~ 1.0 nm/s for EuS and ~ 0.1 nm/s for the Al film. Because Al forms a barrier-type oxide, the samples were stable enough to be handled in air over a period of couple of hours. The samples were mounted in a Quantum Design Physical Properties Measurement System (PPMS) equipped with a He-3 option and a 9 T superconducting solenoid. A breakout box was used to bypass the PPMS electronics so that the sample resistance could be measured with an external lock-in amplifier in a standard four-probe configuration. Voltages in the range of ± 5 V were applied to the gate, which produced corresponding electric fields of ± 1 MV/cm.

We begin by comparing the low temperature transport properties of a pristine 2.6-nm-thick Al film with those of a corresponding EuS/Al bilayer having the same Al layer thickness. As shown in Fig. 2, both the pristine film and the

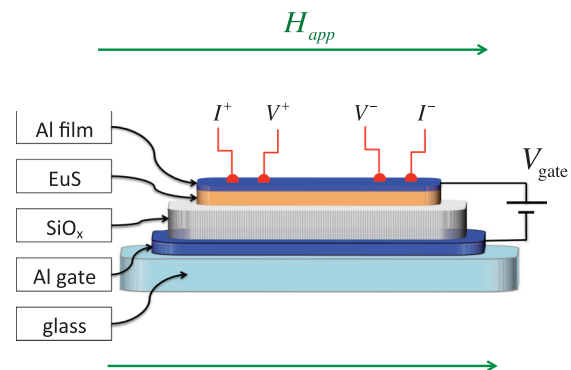


FIG. 1 (color). Schematic diagram of the gated-bilayer geometry. The layer thicknesses are not drawn to scale.

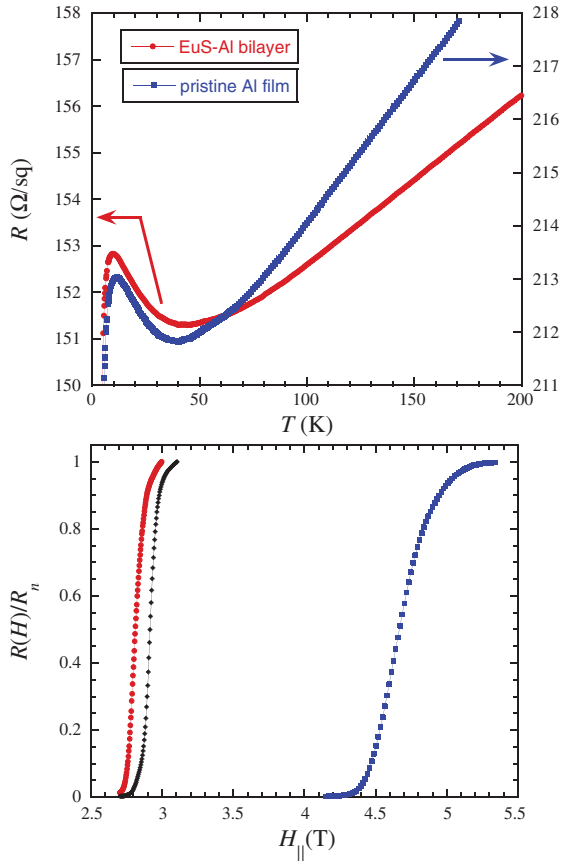


FIG. 2 (color). Upper panel: Sheet resistance as a function of temperature for a pristine 2.6-nm-thick Al film on glass (blue squares) and a bilayer with a 2.6-nm-thick Al film on a 5-nm-thick EuS layer (red circles). Lower panel: The corresponding parallel critical fields for the pristine 2.6-nm-thick Al film on glass (blue squares) and the 2.6 nm Al film on the EuS layer (red circles). Also shown is the critical field transition of a 3.0-nm-thick Al film on EuS. These data were taken at 0.45 K.

bilayer exhibited a low temperature superconducting phase. Although the normal state sheet resistance of both samples was of the same magnitude, the bilayer resistance was about 50% lower than that of the pristine film. Pristine EuS films do not conduct at low temperatures. This suggests that Al deposited on a EuS surface is somewhat less disordered than a comparable Al film deposited directly on glass. The level of disorder for all the bilayers in this study was, in fact, moderate. Their respective sheet resistances fell well below the threshold for strong localization $\hbar/e^2 \sim 26 \text{ k}\Omega$ [17].

In the lower panel of Fig. 2, we show the corresponding parallel critical fields $H_{c\parallel}$ of the two samples, as well as another bilayer sample with a somewhat thicker Al layer (3.0 nm). These data were taken well below the respective zero-field transition temperatures of the Al film and the two bilayers; $T_c = 2.94 \text{ K}$, $T_c = 2.88 \text{ K}$, and $T_c = 2.63 \text{ K}$, respectively. In general, the parallel critical field of a superconducting film whose spin-orbit scattering rate is

low and whose thickness is much less than the coherence length ξ is Zeeman limited and subject to the Clogston-Chandrasekhar (CC) condition: $H_{c\parallel} \approx 1.86T_c$ [18]. Aluminum has a very low spin-orbit scattering rate [19], and for the films in this study, $\xi \sim 15 \text{ nm}$. Therefore, the CC condition was easily met, and, indeed, the critical field of the pristine film in Fig. 2 $H_{c\parallel} = 4.7 \text{ T}$ is in reasonable agreement with the CC limit [20]. In contrast, the apparent critical field of the two bilayers is significantly smaller $H_{c\parallel} \sim 2.8 \text{ T}$, indicating the presence of an exchange field in their respective Al components $H_{\text{ex}} \sim 1.9 \text{ T}$. The measured critical fields of the bilayers are low because their net internal fields are, in fact, somewhat larger than the applied field. This is due to the fact that the internal field has a significant contribution from a proximity-induced exchange field $H_{\text{int}} = H_{\text{app}} + H_{\text{ex}}$. This exchange field is not particular to the EuS-Al interface and has also been observed in EuS/Be bilayers [21] and EuO/Al bilayers [18]. Although the microscopic origins of H_{ex} remain unclear, it is obviously an interface effect. Our primary objective is to modulate the interfacial exchange coupling via an external electric field applied perpendicularly to the EuS-Al interface.

In Fig. 3, we plot the parallel critical field transition of the bilayer of Fig. 2 under various gate voltages V_{gate} at 0.45 K. The application of $\pm 4 \text{ V}$ produces an easily measurable shift in the apparent critical field. The data in Fig. 3 correspond to a 20 mT modulation in the apparent critical field $H_{c\parallel}$. Of course, we believe what is actually being modulated is the exchange field. Similar modulations can be seen in bilayers with varying Al film thicknesses. For instance, in the inset of Fig. 3, we show the modulation of a bilayer with an Al layer thickness of 3 nm. We have also explored ME effects at the midpoint of the critical field transition. In this case, the gate voltage was ramped

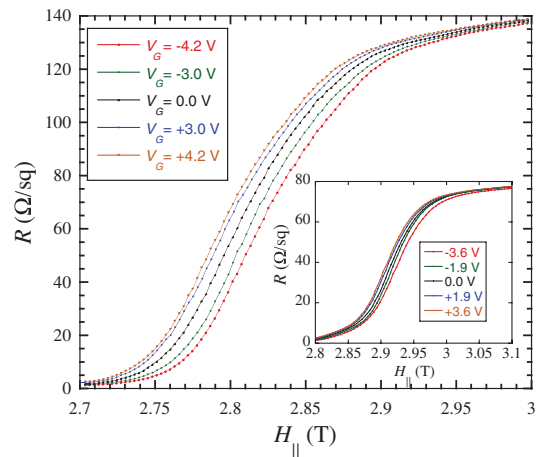


FIG. 3 (color). Parallel critical field transitions of the EuS/Al bilayer in Fig. 2 under various gate voltages at 0.45 K. Inset: Parallel critical field transitions for a bilayer of the same dimensions but with a 3-nm-thick Al layer.

linearly in time between ± 4 V, with the magnetic field set to the midpoint of the transition. Figure 4 shows the resulting time dependence of the bilayer resistance. This oscillation was not observed in the normal state of the bilayer, nor was it observed in pristine Al films of similar thickness. Therefore, the effect cannot be attributed to the carrier modulation of the normal state conductance. Note that the bilayer resistance oscillates symmetrically about the zero voltage value with a magnitude of $\sim 25\%$. If the modulation were, in fact, an electrostrictive effect, or due to heating from a leakage current through the gate barrier, then the modulations would be unilateral about the zero bias resistance. We are confident that with further refinements in sample fabrication, such as using a higher dielectric strength barrier, that we can, in fact, achieve complete switching between the superconducting and normal phases of the Al film, thereby producing a superconducting field-effect transistor.

Although several groups have been successful in switching superconductivity “off and on” with a gate voltage, these efforts have been limited to relatively low carrier density systems [22,23]. Alternatively, our strategy of using a gate to tune the exchange field across the critical field transition of the superconducting film is insensitive to the carrier density. Indeed, with the 50-nm-thick SiO_x barrier used in these studies, the resulting gate-induced charge density modulations were modest. For instance, from the geometry of our samples, we estimate that a gate voltage

of 5 V only produces an excess surface charge density of 2×10^{12} electrons/ cm^2 , which is $\sim 0.01\%$ of the areal free charge density of the 2.6-nm-thick Al layer. This fact is evident in our results for gating experiments on pristine Al films, where we could find no discernible shift in either T_c or the parallel critical field. Indeed, it is well known that it is very difficult to modulate the transition temperature of high carrier-density superconductors with a gate. Glover and Sherrill [24] observed T_c modulations on the order of only 10^{-4} K in tin and indium films using gating fields of comparable magnitude to those of this study.

In the main panel of Fig. 5, we plot the exchange field modulation as a function of the gate electric field for two bilayers of differing Al thickness. Note that the modulation is linear in electric field up to the maximum gate voltages used in this study. We found that the 50-nm-thick SiO_x barrier layer began to break down for gate voltages above ± 5 V; thus, we were limited to electric fields of less than 1 MV/cm. Nevertheless, the data show no obvious signs of saturation, suggesting that much larger modulations could be achieved with a better dielectric barrier. The solid line in Fig. 5 is a linear least-squares fit to the 2.6 nm data. The fit gives a slope of 13 mT per 1 MV/cm of electric field.

In the inset of Fig. 5, we plot ΔH_{ex} , as induced by a 3.6 V gate voltage, as a function of temperature. The modulation decreases rapidly as the temperature is raised above 1 K. Spin resolved tunneling measurements show that the exchange field also decreases significantly over this temperature range [25]. Also shown in the inset of Fig. 5 is the parallel critical field of the bilayer as a function of temperature. Interestingly, its temperature dependence is

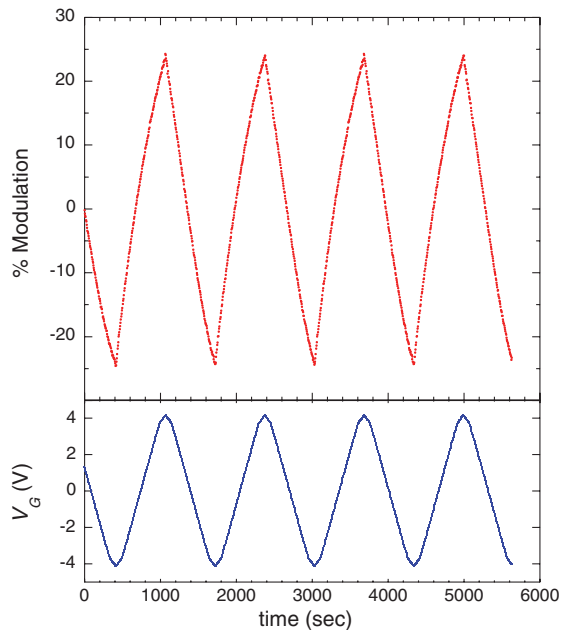


FIG. 4 (color). Upper panel: The time-dependent modulation of the resistance of the bilayer in the main panel of Fig. 2. Lower panel: The corresponding gate voltage as a function of time. The external magnetic field was set to the midpoint of the parallel critical field transition and a sawtoothed voltage waveform applied to the gate. These data were taken at 0.45 K.

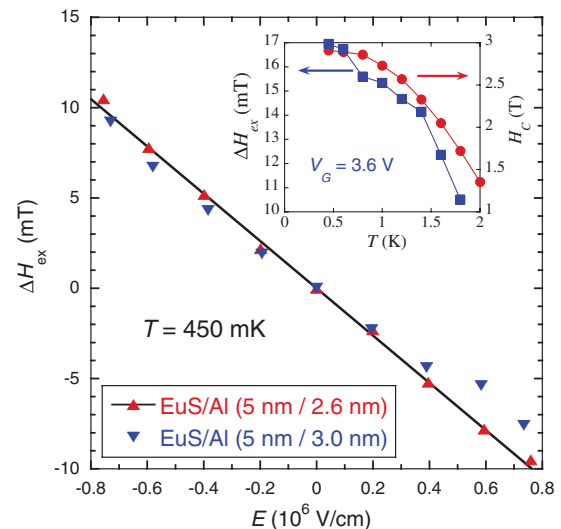


FIG. 5 (color). Electric field shift of the exchange field for the two bilayer samples in Fig. 2. The solid line is a linear least-squares fit to the 2.6 nm data (upward-pointing red triangles). Inset: Magnitude of the exchange field shift induced by a 3.6 V gate voltage as a function of temperature for the 2.6 nm sample. Also plotted is the corresponding temperature dependence of the parallel critical field.

similar to that of the exchange field modulation. The relationship between the condensate and the exchange field remains unclear. Deep in the superconducting phase, i.e., at low temperature and low field, the quasiparticle density is small due to the fact that conduction electrons have been consumed by the formation of the superconducting condensate [26]. This may serve to suppress mechanisms that wash out the exchange field, such as inelastic spin scattering and Fermi liquid effects, thereby producing an enhancement of H_{ex} over the normal state value [21]. Of course, it is also possible that the coupling between the EuS and Al is simply less effective at higher temperatures.

The exchange field originates from interactions between the Al conduction electrons and local magnetic moments in the EuS. However, direct electron conduction in the EuS is not possible due to the band gap, which is $E_g = 1.6$ eV [27]. Of course, the band gap in a thin, disordered EuS film may be somewhat different from the bulk value; nevertheless, electrons in the Al component experience a barrier of the order of ~ 1 eV. We assume that the exchange field is generated in the interfacial region, where the conduction electron wave functions extend into the ferromagnetic environment of the EuS [16,28]. A simple estimate of the characteristic scale of the evanescent tail of a wave function is $\delta \approx \hbar/\sqrt{2mE_g} \approx 0.2$ nm. An external electric field of $E = 10^6$ V/cm will produce a potential gradient of ~ 0.02 V across the interfacial width δ . This value is about 2% of E_g , which corresponds well with the observed few percent modulation of H_{ex} in Fig. 5. So, the ME may arise from the tilting of the barrier over the length scale of the interfacial interaction region. This would also explain why the modulation depends upon the polarity of the gate voltage. For positive (negative) gate voltage, the barrier height is reduced (increased) slightly, thereby increasing (reducing) the conduction electron extension into the ferromagnetic environment of the EuS layer. Of course, we cannot exclude the possibility that interfacial interaction may also be extremely sensitive to changes in the Al surface charge density or the possibility that the disordered EuS layer itself is exhibiting a ME effect. Clearly, a systematic study of ME effects in bilayers comprised of other FIs is needed. For instance, one might replace the EuS layer by EuSe [29] or perhaps EuO [30]. Future studies of the effects of the FI thickness and/or the interface roughness on the exchange field and its corresponding ME behavior should prove enlightening.

In summary, we have demonstrated a novel strategy for producing magnetoelectric effects. In particular, we focus on electric field tuning of the interfacial interaction between the ferromagnetic insulator EuS and superconducting Al films. The strength of exchange can easily be modulated by a few percent with readily attainable gate electric fields. In principle, one should be able to optimize this ME effect by using high dielectric constant barriers and/or improving the interface quality. The ultimate goal

would be to realize a device such as a voltage-controlled superconducting switch or a spin-polarized electron source with a voltage-tunable Zeeman splitting.

We thank Ilya Vekhter and Gianluigi Catelani for enlightening discussions. We are also indebted to Jayne Garno, Cha Marra, and Xianglin Zhai for atomic force microscopy images of our samples. This work was supported by the DOE under Grant No. DE-FG02-07ER46420.

-
- [1] C.H. Ahn, J.M. Triscone, and J. Mannhart, *Nature (London)* **424**, 1015 (2003).
 - [2] I. Zutic, J. Fabian, and S.D. Sarma, *Rev. Mod. Phys.* **76**, 323 (2004).
 - [3] C.H. Ahn *et al.*, *Rev. Mod. Phys.* **78**, 1185 (2006).
 - [4] T. Dietl, *Nat. Mater.* **9**, 965 (2010).
 - [5] H. Ohno, *Nat. Mater.* **9**, 952 (2010).
 - [6] W. Eerenstein, N.D. Mathur, and J.F. Scott, *Nature (London)* **442**, 759 (2006).
 - [7] V. Laukhin *et al.*, *Phys. Rev. Lett.* **97**, 227201 (2006).
 - [8] J.P. Velev, S.S. Jaswal, and E.Y. Tsymlal, *Phil. Trans. R. Soc. A* **369**, 3069 (2011).
 - [9] H. Ohno, D. Chiba, F. Matsukura, T. Omiya, E. Abe, T. Dietl, Y. Ohno, and K. Ohtani, *Nature (London)* **408**, 944 (2000).
 - [10] D. Chiba, M. Sawicki, Y. Nishitani, Y. Nakatani, F. Matsukura, and H. Ohno, *Nature (London)* **455**, 515 (2008).
 - [11] I.M. Miron, G. Gaudin, S. Auffret, B. Rodmacq, A. Schuhl, S. Pizzini, J. Vogel, and P. Gambardella, *Nat. Mater.* **9**, 230 (2010).
 - [12] D.C. Ralph and M.D. Stiles, *J. Magn. Magn. Mater.* **320**, 1190 (2008).
 - [13] S.M. Wu, S.A. Cybart, D. Yi, J.M. Parker, R. Ramesh, and R.C. Dynes, *Phys. Rev. Lett.* **110**, 067202 (2013).
 - [14] G. Sarma, *J. Phys. Chem. Solids* **24**, 1029 (1963).
 - [15] P.G. De Gennes, *Phys. Lett.* **23**, 10 (1966).
 - [16] J.S. Moodera, T.S. Santos, and T. Nagahama, *J. Phys. Condens. Matter* **19**, 165202 (2007).
 - [17] V. Yu. Butko and P.W. Adams, *Nature (London)* **409**, 161 (2001).
 - [18] R. Meservey and P.M. Tedrow, *Phys. Rep.* **238**, 173 (1994).
 - [19] X.S. Wu, P.W. Adams, Y. Yang, and R.L. McCarley, *Phys. Rev. Lett.* **96**, 127002 (2006).
 - [20] V. Yu. Butko, P.W. Adams, and E.I. Meletis, *Phys. Rev. Lett.* **83**, 3725 (1999).
 - [21] T.J. Liu, J.C. Prestigiacomo, Y.M. Xiong, and P.W. Adams, *Phys. Rev. Lett.* **109**, 147207 (2012).
 - [22] C.H. Ahn, S. Gariglio, P. Paruch, T. Tybell, L. Antognazza, and J.-M. Triscone, *Science* **284**, 1152 (1999).
 - [23] K.A. Parendo, K.H.S.B. Tan, A. Bhattacharya, M. Eblen-Zayas, N.E. Staley, and A.M. Goldman, *Phys. Rev. Lett.* **94**, 197004 (2005); X. Leng, J. Garcia-Barriocanal, S. Bose, Y. Lee, and A.M. Goldman, *Phys. Rev. Lett.* **107**, 027001 (2011).
 - [24] R.E. Glover, III and M.D. Sherrill, *Phys. Rev. Lett.* **5**, 248 (1960).

- [25] Y.M. Xiong, S. Stadler, P.W. Adams, and G. Catelani, *Phys. Rev. Lett.* **106**, 247001 (2011).
- [26] G. Catelani, X. S. Wu, and P.W. Adams, *Phys. Rev. B* **78**, 104515 (2008).
- [27] A. Mauger and C. Godart, *Phys. Rep.* **141**, 51 (1986).
- [28] G.M. Roesler, M.E. Filipkowski, P.R. Broussard, Y.U. Idzerda, M.S. Osofsky, R.J. Soulen, Jr., and I. Bozovic, *Proc. SPIE Int. Soc. Opt. Eng.* **2157**, 285 (1994).
- [29] R.T. Lechner, G. Springholz, T.U. Schulli, J. Stangl, T. Schwarzl, and G. Bauer, *Phys. Rev. Lett.* **94**, 157201 (2005).
- [30] L. Passell, O. W. Dietrich, and J. Als-Nielsen, *Phys. Rev. B* **14**, 4897 (1976).